

Orientational Phase Transition of Microtubules in 3D Using Mean-Field Theory

Cameron Gibson¹, Tamsin A. Spelman¹, Henrik Jönsson^{1,2,3}

¹ Sainsbury Laboratory, Cambridge University, Bateman Street,
Cambridge CB2 1LR, UK

²Department of Applied Mathematics and Theoretical Physics
(DAMTP), University of Cambridge, Cambridge, UK

³Computational Biology and Biological Physics, Lund University,
Sölvegatan 14A, 223 62 Lund, Sweden

For Correspondence:

cameron.gibson@slcu.cam.ac.uk, henrik.jonsson@slcu.cam.ac.uk

March 13, 2022

Abstract

Microtubules (MTs) are active fibres which form one part of a plant cell cytoskeleton, and have been observed experimentally to undergo spontaneous self-alignment. Here, we derive a 3D mean-field theory to analyse the orientational phase transition of microtubules nucleating and growing within 3D space. We identify a control parameter, dependent on microtubule properties, and calculate the value of the control parameter for which a phase transition is possible.

1 Introduction

Microtubules are polymers of tubulin that form an active fibre network in all eukaryotic cells [1]. In plant cells, together with actin microfilaments, they form the cytoskeleton [2, 3]. The cytoskeleton is vital in plant cells for cell division, expansion, and morphogenesis [4, 5, 6]. Each microtubule has a plus end and a minus end which both either grow or shrink via the assembly and disassembly of tubulin [7]. For our model, we assume that the minus end is static since it changes at a much slower rate than the plus end [8].

Microtubule networks exhibit similarities with the condensed matter system of nematic liquid crystals [9, 10] which can be viewed as a system of many hard interacting rods. Furthermore, high levels of spontaneous alignment have been observed experimentally in microtubule systems which are qualitatively similar to phase transitions in nematic liquid crystals [11]. Various models have been proposed to analyse cytoskeletal dynamics [12, 13, 14, 15]. A useful analytical (continuum theory) approach is mean-field theory [16], which is often used to analyse condensed matter systems and to analyse microtubule dynamics [17, 18, 19, 20, 21].

In [20], a 2D mean-field theory model for microtubule dynamics was analysed, but excluding any catastrophe dynamics, which refers to a growing microtubule spontaneously switching to shrinking in response to collision with another microtubule. These catastrophe dynamics were included in the model of [21], where they formulated a 2D mean-field theory of microtubules and proved the existence of a phase transition. In this paper, we extend the 2D model in [21] to 3D in a novel way, highlighting the differences and similarities between the two cases as well as proving the existence of a physically realisable phase transition in 3D.

This paper is organised as follows. In Section 2, we set up the 3D equations governing the system and solve them in the isotropic case. In Section 3, we make a comparison with the 2D case in Subsection 3.1 and then numerically determine constraints on our system that allow for a phase transition to occur in 3D in Subsection 3.2.

2 Model

Here, we will outline our model. Note that, we will use spherical polar coordinates to describe directions in 3D space, denoted by (θ, ϕ) and use the convention that θ and ϕ are the polar and azimuthal angles respectively. When comparing to the 2D case, we will similarly use the 2D polar coordinate θ to describe direction in 2D space.

2.1 Assumptions

In this subsection, we state the key assumptions that we make about our system of microtubules.

Firstly, we assume that microtubules nucleate everywhere in 3D space at a constant rate $\frac{r_n}{4\pi}$, are static at the minus end, and are either growing or shrinking at the plus end with speed v^+ or v^- respectively. The plus end can switch from shrinking to growing via spontaneous rescue with rate r_r and switch from shrinking to growing via spontaneous catastrophe with rate r_c .

We assume that microtubules grow in a straight line, with some probability of changing direction when two microtubules collide in a process called zippering. The microtubules grow (and shrink) in segments, with joints allowing each segment to be oriented in a different direction. Specifically, when a growing segment collides with a second segment, either there is an induced catastrophe (it starts shrinking), crossover (it keeps growing unhindered) or zippering (it starts growing in direction of the second segment) with respective probabilities $P_c(\sigma)$, $P_x(\sigma)$ and $P_z(\sigma)$ all written as functions of the collision angle σ .

2.2 Master Equations

In this subsection, we determine the differential equations governing the physical system. For further details, see [21] where the similar 2D equations are derived.

We assume that the density of microtubule is large enough so that we can work with a continuum theory, allowing us to define a macroscopic description of the system. Therefore, we define $m_i^{+/-/0}(l, \theta, \phi, t)$ as the density of microtubule segments in direction (θ, ϕ) of length l at time t with $+/-/0$ indicating a growing/shrinking/inactive segment and i indexing the segments (letting $i = 1$ index the first segment).

Then, the master equations governing the evolution of our system can be expressed in terms of flux terms denoted Φ_{event} .

$$\begin{aligned} \partial_t m_i^+(l_i, \theta_i, \phi_i, t) &= \Phi_{growth} + \Phi_{rescue} - \Phi_{spontcat} - \Phi_{inducedcat} - \Phi_{zipper}, \\ \partial_t m_i^-(l_i, \theta_i, \phi_i, t) &= \Phi_{shrinkage} - \Phi_{rescue} + \Phi_{spontcat} + \Phi_{inducedcat} \\ &\quad + \Phi_{reactivation}, \\ \partial_t m_i^0(l_i, \theta_i, \phi_i, t) &= \Phi_{zipper} - \Phi_{reactivation}. \end{aligned} \tag{2.1}$$

There is the flux term $\Phi_{growth} \equiv -v^+ \partial_{l_i} m_i^+(l_i, \theta_i, \phi_i, t)$ derived from $-v^+ \partial_{l_i} m_i^+ = \frac{\partial_{l_i}}{\partial t} \partial_t m_i^+ = \partial_{l_i} m_i^+$ and the flux term $\Phi_{shrinkage} \equiv v^- \partial_{l_i} m_i^-(l_i, \theta_i,$

$\phi_i, t)$ derived from $v^- \partial_{l_i} m_i^- = \frac{\partial_{l_i}}{\partial t} \partial_t m_i^- = \partial_{l_i} m_i^-$. The flux terms $\Phi_{rescue} \equiv r_r m_i^-(l_i, \theta_i, \phi_i, t)$ and $\Phi_{spontcat} \equiv r_c m_i^+(l_i, \theta_i, \phi_i, t)$ arise from spontaneous rescue and spontaneous catastrophe respectively.

There is the flux term $\Phi_{reactivation} \equiv \int d\theta_{i+1} \int d\phi_{i+1} \sin(\theta_{i+1}) m_{i+1}^-(l_i = 0, \theta_{i+1}, \phi_{i+1}, t) p_{unzip}(\theta_i, \phi_i, l_i | \theta_{i+1}, \phi_{i+1}, t)$ where $p_{unzip}(\theta_i, \phi_i, l_i | \theta_{i+1}, \phi_{i+1}, t)$ is the probability that the $(i+1)^{th}$ segment shrinks from the direction $(\theta_{i+1}, \phi_{i+1})$ to length zero at time t and reactivates the i^{th} segment of length l_i in direction (θ_i, ϕ_i) . Detailed arguments as to why p_{unzip} is already determined by our previous assumptions are given in [21], which carry over from 2D to 3D.

Let $k(\theta, \phi, t) \equiv \sum_i \int dl_i l_i (m_i^+(l_i, \theta, \phi, t) + m_i^-(l_i, \theta, \phi, t) + m_i^0(l_i, \theta, \phi, t))$ be the length density of microtubules pointing in direction (θ, ϕ) . We can then consider the induced catastrophe flux term

$$\Phi_{inducedcat} \equiv v^+ m_i^+(l_i, \theta_i, \phi_i, t) \int d\theta' \int d\phi' \sin(\theta') c(\theta_i - \theta', \phi_i, \phi') k(\theta', \phi', t). \quad (2.2)$$

where, in 3D, we define

$$c(\theta, \theta', \phi - \phi') \equiv |\sin(\sigma)| P_c(\sigma(\theta, \theta', \phi - \phi')), \quad (2.3)$$

and also define

$$\sigma = \arccos(\sin(\theta) \sin(\theta') \cos(\phi - \phi') + \cos(\theta) \cos(\theta')). \quad (2.4)$$

as the angle between the two directions (θ, ϕ) and (θ', ϕ') . The $|\sin|$ term in Eq. 2.3 compensates for the fact that the probability of collision will change with the angle between interacting segments. For example, perpendicular segments will always collide and parallel segments will always collide. Φ_{zipper} is defined similarly as $\Phi_{inducedcat}$ is in Eq. 2.2 but with c replaced by z .

2.3 Control Parameter

An important parameter in our system is $g = \frac{r_r}{v^-} - \frac{r_c}{v^+}$ [20, 21]. Physically, g corresponds to the non-interacting behaviour of the microtubules. $g \rightarrow -\infty$ corresponds to a completely catastrophic system, which is trivially isotropic. $g \rightarrow \infty$ corresponds to an overwhelmingly growing system, which is trivially anisotropic. Following our earlier analogy of expecting a phase transition in a liquid crystal system, we identify g as our control parameter, which is analogous to temperature in liquid crystals. Therefore, we expect there to be an orientational phase transition as we increase g from negative infinity. We also note that the only physically realisable values of g are negative, since positive g corresponds to unbounded growth.

2.4 Steady State System

In this subsection, we write down the equations describing the steady state system that arise from the master equations Eq. 2.1. A complete derivation of steady state equations for the 2D system is given in [21].

We define $l(\theta, \phi)$ to be the average segment length in the direction (θ, ϕ) :

$$\frac{1}{l(\theta_i, \phi_i)} = -g + \int d\theta' \int d\phi' \sin(\theta') [c(\theta_i, \theta', \phi_i - \phi') + z(\theta_i, \theta', \phi_i - \phi')] k(\theta', \phi'). \quad (2.5)$$

We define $Q(\theta, \phi)$ as the ratio of inactive to active (both growing and shrinking) segments in the direction (θ, ϕ) :

$$Q(\theta, \phi) = \frac{m^0(\theta, \phi)}{m^+(\theta, \phi) + m^-(\theta, \phi)}. \quad (2.6)$$

We define $t(\theta, \phi)$ to be the density of active segments in the direction (θ, ϕ) :

$$t(\theta, \phi) = \left(1 + \frac{v^+}{v^-}\right) l(\theta, \phi) \sum_{i=1}^{\infty} m_i(\theta, \phi). \quad (2.7)$$

For convenience, we define dimensionless quantities by first defining a variable l_0 with dimensions of length.

$$l_0 = \left[\left(\frac{1}{v^+} + \frac{1}{v^-} \right) \frac{r_n}{4\pi} \right]^{-\frac{1}{4}}. \quad (2.8)$$

Our dimensionless quantities are then $G = gl_0^{\frac{4}{3}}$, $L = ll_0^{-\frac{4}{3}}$, $K = kl_0^{\frac{4}{3}}$ and $T = tl_0^{\frac{8}{3}}$.

Even though it has been made dimensionless, G is still the control parameter of our system:

$$G = \left[\frac{2v^+v^-}{r_n(v^+ + v^-)} \right]^{\frac{1}{4}} \left(\frac{r_r}{v^-} - \frac{r_c}{v^+} \right). \quad (2.9)$$

We also summarise expressions like Eq. 2.2 by defining the dimensionless functionals:

$$F[h](\theta, \phi) = \int_0^\pi d\theta' \int_0^{2\pi} d\phi' \sin(\theta') f(\theta, \theta', \phi - \phi') h(\theta', \phi') \quad \text{for } F \in [C, Z]. \quad (2.10)$$

The steady state 3D equations are then the following:

$$\begin{aligned}\frac{1}{L(\theta, \phi)} &= -G + C[K](\theta, \phi) + Z[K](\theta, \phi), \\ K(\theta, \phi) &= L(\theta, \phi)(1 + Q(\theta, \phi))T(\theta, \phi), \\ Q(\theta, \phi) &= Z[LK(1 + Q)](\theta, \phi), \\ T(\theta, \phi) &= L(\theta, \phi) + L(\theta, \phi)K(\theta, \phi)Z[T](\theta, \phi).\end{aligned}\tag{2.11}$$

2.5 Isotropic Solution

In this subsection, we consider the isotropic case of the steady state 3D equations Eq. 2.11, then solve this system.

The spherical harmonics [22, 23] are a complete set of orthogonal functions $Y_\ell^m : S^2 \rightarrow \mathbb{R}$ with two indices (ℓ and m) that can be defined in the following way. Note that we have chosen them to be real-valued functions.

$$Y_\ell^m(\theta, \phi) = \begin{cases} (-1)^m \sqrt{2} \sqrt{\frac{2\ell+1}{4\pi} \frac{(\ell-|m|)!}{(\ell+|m|)!}} P_\ell^{|m|}(\cos(\theta)) \sin(|m|\phi) & \text{if } m < 0, \\ \sqrt{\frac{2\ell+1}{4\pi}} P_\ell^m(\cos(\theta)) & \text{if } m = 0, \\ (-1)^m \sqrt{2} \sqrt{\frac{2\ell+1}{4\pi} \frac{(\ell-m)!}{(\ell+m)!}} P_\ell^{|m|}(\cos(\theta)) \cos(m\phi) & \text{if } m > 0. \end{cases}\tag{2.12}$$

Here, P_ℓ^m are the associated Legendre polynomials, defined in terms of the standard Legendre polynomials P_ℓ :

$$P_\ell^m(\cos \theta) = (-1)^m (\sin \theta)^m \frac{d^m}{d(\cos \theta)^m} (P_\ell(\cos \theta)).\tag{2.13}$$

$$P_\ell(x) = \frac{1}{2^\ell \ell!} \frac{d^\ell}{dx^\ell} (x^2 - 1)^\ell.\tag{2.14}$$

The spherical harmonics given by Eq. 2.12 provide an orthonormal basis of eigenfunctions of Eq. 2.10. To prove this, we first make a change of variables in Eq. 2.10 via $f(\sigma) \equiv \mathfrak{F}(\cos(\sigma))$ with $f \in [c, z]$ and $\mathfrak{F} \in [\mathfrak{C}, \mathfrak{Z}]$ respectively, and with σ defined by Eq. 2.4. We then make a Legendre expansion

$$\mathfrak{F}(\cos(\sigma)) = \sum_{\ell=0}^{\infty} \mathfrak{F}_\ell P_\ell(\cos(\sigma))\tag{2.15}$$

$$\text{where } \mathfrak{F}_\ell = \frac{2\ell+1}{2} \int_{-1}^1 \mathfrak{F}(x) P_\ell(x) dx.\tag{2.16}$$

Then, using the spherical harmonic addition theorem $P_\ell(\cos(\sigma)) = \frac{4\pi}{2\ell+1} \sum_{m=-\ell}^{\ell} Y_\ell^m(\theta, \phi) Y_\ell^{m*}(\theta', \phi')$ [22, 23], we rewrite Eq. 2.15 and substitute this into Eq. 2.10. Finally, we simplify with the standard orthogonality condition

of spherical harmonics $\int_0^\pi d\theta' \int_0^{2\pi} d\phi' Y_\ell^m(\theta', \phi') Y_{\ell'}^{m'}(\theta', \phi') = \delta_{\ell\ell'} \delta^{mm'}$, which leaves us with

$$F[Y_\ell^m(\theta, \phi)] = \frac{4\pi\mathfrak{F}_\ell}{2\ell+1} Y_\ell^m(\theta, \phi). \quad (2.17)$$

We now use Eq. 2.17 with $\ell = m = 0$ to give us $F[1] = 4\pi\mathfrak{F}_0$. In the isotropic (and stationary) state of the system, all angular dependence drops out of our variables, which we reflect with an overbar, and our system of equations becomes

$$\begin{aligned} \frac{1}{\bar{L}} &= -G + (4\pi\mathfrak{C}_0 + 4\pi\mathfrak{Z}_0)\bar{K} \\ \bar{K} &= \bar{L}(1 + \bar{Q})\bar{T} \\ \bar{Q} &= 4\pi\mathfrak{Z}_0\bar{L}\bar{K}(1 + \bar{Q}) \\ \bar{T} &= \bar{L} + 4\pi\mathfrak{Z}_0\bar{L}\bar{K}\bar{T}. \end{aligned} \quad (2.18)$$

Eq. 2.18 together imply the following relation:

$$\bar{K}(4\pi\mathfrak{C}_0\bar{K} - G)^2 = 1. \quad (2.19)$$

This relation implies that, given one of \bar{K} and G , there is a unique solution for the other if $\mathfrak{C}_0 > 0$ (since we must have a non-negative density \bar{K}). We will consider a positive value of \mathfrak{C}_0 that reasonably matches experiment in Subsection 3.2.

Note that all graphing in this paper in the subsequent section is done using MATLAB R2021b.

3 Results

3.1 Comparison to 2D System

Here, we compare our 3D model to the 2D model of [21]. An important similarity is that we have the same definition of our control parameter $g = \frac{r_c}{v^-} - \frac{r_r}{v^+}$.

There, however, is a difference in how Eq. 2.2 is defined, with the implicit factor adjusting for varying collision probability being $|\sin(\sigma)|$ with $\sigma = \arccos(\sin(\theta)\sin(\theta')\cos(\phi - \phi') + \cos(\theta)\cos(\theta'))$ in 3D instead of $|\sin(\theta)|$ in 2D.

Furthermore, there are differences in the definition of l_0 in Eq. 2.8 as well as the factors of l_0 involved in forming dimensionless quantities.

Subsection 2.5 is very different from the 2D model. Fourier modes form an orthonormal basis of eigenfunctions for the 2D version of Eq. 2.10, instead of spherical harmonics in the 3D model. As a result, Eq. 2.18 and Eq. 2.19 then involve Legendre coefficients in 3D instead of Fourier coefficients in 2D.

3.2 First Order Perturbation

In this subsection, we consider the constraints on our system for a physically realisable change in microtubule alignment to occur.

In order to reach an ordered state from the isotropic state (i.e. undergo a phase transition), the system has to undergo a small perturbation first. Therefore, we define small perturbations $\lambda, \kappa, \chi, \tau$ to the variables in our system via

$$L = \bar{L}(1 + \lambda), \quad K = \bar{K}(1 + \kappa), \quad Q = \bar{Q}(1 + \chi) \quad \text{and} \quad T = \bar{T}(1 + \tau). \quad (3.1)$$

Following the 2D case in [21], we require that Eq. 2.18 holds to first order in $\lambda, \kappa, \chi, \tau$ then put each side of the second of these first order equations as the functional argument of $Z[\]$. Then, after a linear rearrangement of the resulting equations, we get the eigenvalue equation

$$(1 - 4\pi\mathfrak{Z}_0\bar{N})\kappa = -2\bar{N}C[\kappa]. \quad (3.2)$$

where $\bar{N} = \bar{L}\bar{K}$. Recognising this as a special case of Eq. 2.17 gives us the spherical harmonics defined in Eq. 2.12 as an orthonormal basis of eigenfunctions for this eigenvalue equation. Therefore, we have a set of potential values of \bar{N} for which a phase transition is possible, which we denote as $\bar{N}_\ell^* = (4\pi\mathfrak{Z}_0 - \frac{8\pi}{2\ell+1}\mathfrak{C}_\ell)^{-1}$, with the index ℓ corresponding to the lower index of the spherical harmonics, since the eigenvalues in Eq. 2.17 do not depend on the upper index. Eq. 2.18 then implies that these values of \bar{N} correspond to values of G , which we write as

$$G^* = \left[1 + \frac{(2\ell+1)\mathfrak{C}_0}{2\mathfrak{C}_\ell} \right] \left[-\frac{8\pi\mathfrak{C}_\ell}{2\ell+1} \right]^{\frac{1}{3}}. \quad (3.3)$$

As in 2D case, our model predicts that the location of a possible phase transition depends on P_c and not on P_z , since there is no dependence on \mathfrak{Z}_l in Eq. 3.3.

We choose P_c to be a linear function (as a function of collision angle), increasing linearly from $(0, 0)$ to $(\frac{\pi}{2}, \frac{\pi}{4})$ then decreasing linearly back down to $(\pi, 0)$, in order to reasonably match experimental data for P_c [24]. This is plotted in Figure 1. We can then numerically calculate

$$\mathfrak{C}_\ell = \frac{2\ell+1}{2} \int_0^\pi \sin^2(y) P_\ell(y) P_\ell(\cos(y)) dy \quad (3.4)$$

which is obtained from Eq 2.16 through the change of variables $x = \cos(y)$. Due to P_ℓ being an odd function for odd ℓ , the integrand is odd about $\frac{\pi}{2}$ and so $\mathfrak{C}_\ell = 0$ for odd ℓ . The values of \mathfrak{C}_ℓ are plotted numerically for

$\ell = 0, 2, \dots, 200$ in Figure 2. The corresponding values of G^* are plotted in Figure 3 using Eq. 3.3. As discussed in 2.3, only negative values of G correspond to physically realisable solutions with bounded growth, so it is promising that all plotted values of G^* are negative. We now must identify which G^* corresponds to a physical perturbation of the system. Without further analysis, we might conclude that all these values of G^* correspond to physically realisable phase transitions. However, we need to consider whether the order of the system can actually be changed by the perturbations we are considering.

Following our earlier comparison to nematic liquid crystals, we use the nematic order parameter [9, 10, 25] to quantify the alignment in our system. In d dimensions, this is a unique tensor up to an overall factor, which we set to unity in the completely anisotropic state.

$$S_{ab} = \left\langle \frac{d}{d-1} n_a n_b - \frac{1}{d-1} \delta_{ab} \right\rangle, \quad (3.5)$$

where $\langle \rangle$ denotes taking an average over all microtubules, which each has a unit vector n_a describing their direction. Therefore, in 3D, we have the 3x3 matrix

$$S = \frac{\int_0^\pi d\theta \int_0^{2\pi} d\phi \sin(\theta) K(\theta, \phi) \left(\frac{3}{2} n \otimes n - \frac{1}{2} \mathcal{I} \right)}{\int_0^\pi d\theta \int_0^{2\pi} d\phi \sin(\theta) K(\theta, \phi)}. \quad (3.6)$$

S has three eigenvalues: these are all zero if and only if the system is in the completely isotropic case. Therefore, we shall analyse when S has non-zero eigenvalues, which corresponds to a non-isotropic state.

To evaluate whether the spherical harmonic perturbations change the order of the system, for every value of ℓ , we take κ to be each of the $2\ell + 1$ spherical harmonics (here, real and normalised) and calculate the maximum and minimum eigenvalues of the resulting 3D nematic order parameter S . This is plotted in Figure 4a. This shows that only \mathfrak{C}_2 corresponds to a non-zero S (within numerical accuracy) and therefore allows a phase transition. If all perturbations could cause a phase transition, then a negligible change in some value of \mathfrak{C}_l for some high l could drastically change the system whilst barely changing $P_c(\theta)$ at all. However, since this is not the case, we can focus on \mathfrak{C}_2 and ignore the higher Legendre modes. Since Eq. 3.1 is only valid when the perturbation κ is small, we repeat our calculation with each spherical harmonic perturbation divided by 100 to check that what we have done is valid for small κ . We can see in Figure 4b that we still get a change in the order parameter for a smaller perturbation (although as we might expect the change in order parameter eigenvalues is smaller).

Therefore, we have $G^* = -1.56$ (3sf), which corresponds to \mathfrak{C}_2 , as the prediction for the value of the control parameter for which a phase transition

is possible. For this value of G , when the density of microtubules $K(\theta, \phi)$ is perturbed slightly from its isotropic value by a $l = 2$ spherical harmonic, a phase transition is possible.

4 Conclusion

In this paper, we have developed a 3D mean-field theory for an interacting system of microtubules. Furthermore, if we take the probability of induced catastrophe to be a linear function of collision angle, which approximates experimental data [24], we numerically find one physically realisable value of G^* for which there is a change of the order parameter from its isotropic value. Physically, this corresponds to the constraint $G^* = -1.56$ (3sf), which is the threshold for microtubules to change from a disordered to ordered state.

Acknowledgements All three authors acknowledge support from the Gatsby Charitable Foundation (GAT3395/PR4B) and additionally T.A.S and H.J acknowledge support from the Human Frontier Science Program Organization (Grant RGP0009/2018).

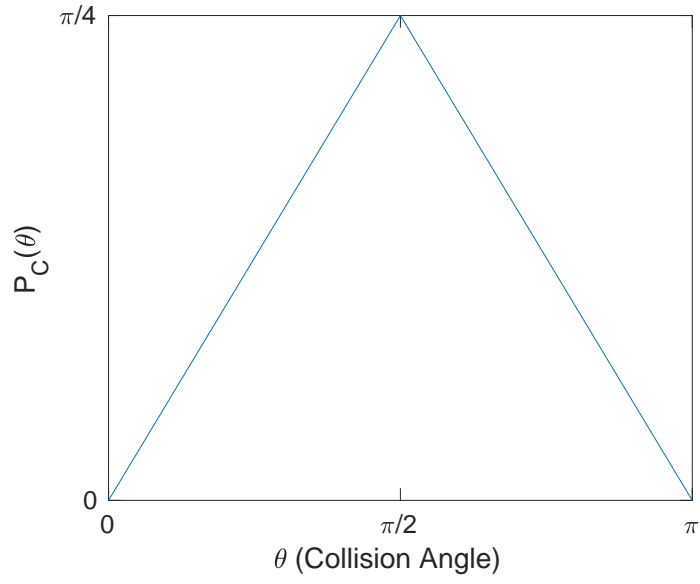


Figure 1: Probability of induced catastrophe as a function of collision angle between two interacting microtubules. This is chosen to approximately match experimental results [24].

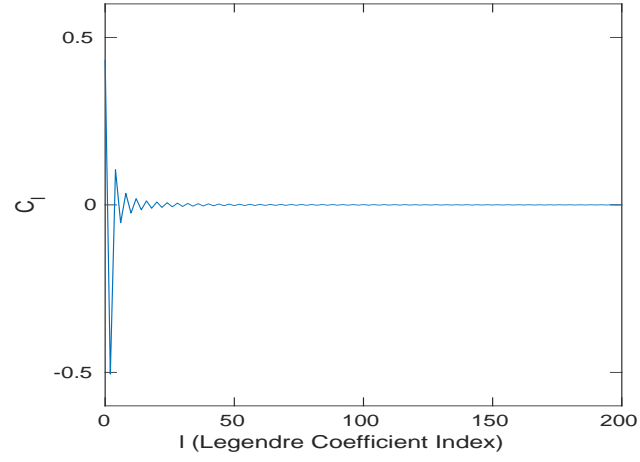


Figure 2: The Legendre coefficients \mathfrak{C}_l are plotted for $\ell = 0, 2, \dots, 200$ using Eq. 3.4.

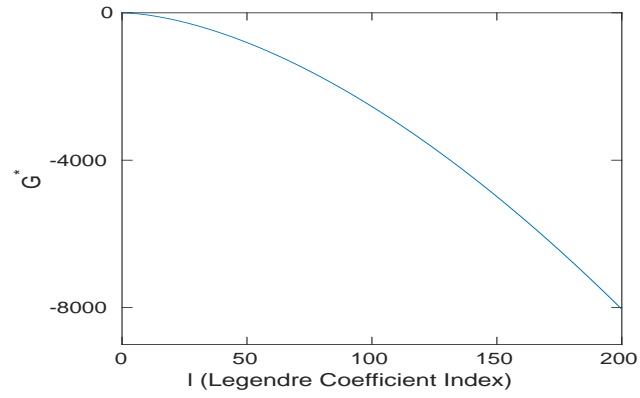
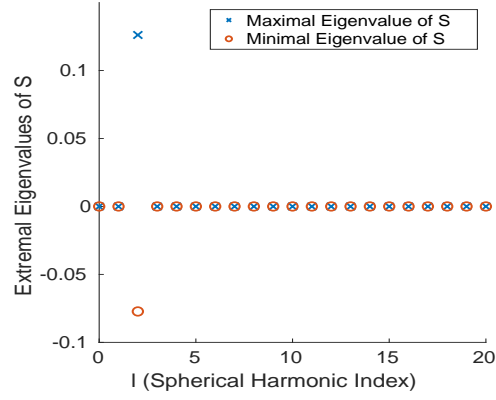
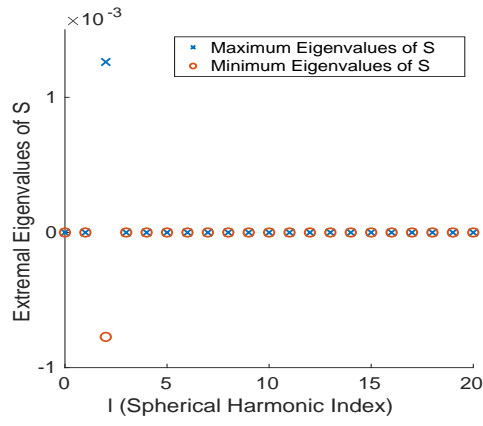


Figure 3: Values G^* of the control parameter G that correspond to a system allowing the existence of a phase transition. G depends on l through Eq. 3.3 and we plot values corresponding to $l = 0, 2, \dots, 200$.



(a)



(b)

Figure 4: Maximum and minimum eigenvalues of the 3D order parameter S are plotted against the spherical harmonic index ℓ of the perturbation κ .
(a) The $\ell = 2$ spherical harmonics are singled out as the only perturbations to change the order of the system.
(b) Similar result with spherical harmonic perturbations divided by 100.

References

- [1] Richard Wade. On and around microtubules: An overview. *Molecular biotechnology*, 43:177–91, 07 2009.
- [2] R. H. Goddard, S. M. Wick, C. D. Silflow, and D. P. Snustad. Microtubule Components of the Plant Cell Cytoskeleton. *Plant Physiology*, 104(1):1–6, 01 1994.
- [3] Daniel A. Fletcher and R. Dyche Mullins. Cell mechanics and the cytoskeleton. *Nature*, 463:485–492, 2010.
- [4] Carolyn G. Rasmussen, Amanda J. Wright, and Sabine Müller. The role of the cytoskeleton and associated proteins in determination of the plant cell division plane. *The Plant Journal*, 75(2):258–269, 2013.
- [5] Logan Bashline, Lei Lei, Shundai Li, and Ying Gu. Cell wall, cytoskeleton, and cell expansion in higher plants. *Molecular Plant*, 7(4):586–600, 2014.
- [6] Whitney E. Hable, Sherryl R. Bisgrove, and Darryl L. Kropf. To Shape a Plant—The Cytoskeleton in Plant Morphogenesis. *The Plant Cell*, 10(11):1772–1774, 11 1998.
- [7] Gary J. Brouhard. Dynamic instability 30 years later: complexities in microtubule growth and catastrophe. *Molecular Biology of the Cell*, 26(7):1207–1210, 2015. PMID: 25823928.
- [8] Anna Akhmanova and Michel O. Steinmetz. Microtubule minus-end regulation at a glance. *Journal of Cell Science*, 132(11), 06 2019. jcs227850.
- [9] Pierre de and Jacques Prost. *The Physics of Liquid Crystal*, volume 2. Oxford University Press, 01 1993.
- [10] Denis Andrienko. Introduction to liquid crystals. *Journal of Molecular Liquids*, 267:520–541, 2018.
- [11] Anne L Hitt, Alan R. Cross, and Robley Cook Williams. Microtubule solutions display nematic liquid crystalline structure. *The Journal of biological chemistry*, 265 3:1639–47, 1990.
- [12] Edith Geigant, Karina Ladizhansky, and Alexander Mogilner. An integro-differential model for orientational distributions of f-actin in cells. *SIAM J. Appl. Math.*, 59:787–809, 1997.
- [13] Igor S. Aranson and Lev S. Tsimring. Theory of self-assembly of microtubules and motors. *Phys. Rev. E*, 74:031915, Sep 2006.

- [14] V Rühle, Falko Ziebert, R Peter, and Walter Zimmermann. Instabilities in a two-dimensional polar-filament-motor system. *The European physical journal. E, Soft matter*, 27:243–51, 11 2008.
- [15] Shantia Yarahmadian and Masoud Yari. Phase transition analysis of the dynamic instability of microtubules. *Nonlinearity*, 27, 10 2013.
- [16] P. M. Chaikin and T. C. Lubensky. *Mean-field theory*, page 144–212. Cambridge University Press, 1995.
- [17] Marileen Dogterom and Stanislas Leibler. Physical aspects of the growth and regulation of microtubule structures. *Phys. Rev. Lett.*, 70:1347–1350, Mar 1993.
- [18] Adam R Lamson, Jeffrey M. Moore, Fang Fang, Matthew A. Glaser, Michael J. Shelley, and Meredith D. Betterton. Comparison of explicit and mean-field models of cytoskeletal filaments with crosslinking motors. *The European Physical Journal E*, 44:1–22, 2021.
- [19] Xia-qing Shi and Yu-qiang Ma. Understanding phase behavior of plant cell cortex microtubule organization. *Proceedings of the National Academy of Sciences*, 107(26):11709–11714, 2010.
- [20] Vladimir A. Baulin, Carlos M. Marques, and Fabrice Thalmann. Collision induced spatial organization of microtubules. *Biophysical Chemistry*, 128(2):231–244, 2007.
- [21] Rhoda J. Hawkins, Simon H. Tindemans, and Bela M. Mulder. Model for the orientational ordering of the plant microtubule cortical array. *Phys. Rev. E*, 82:011911, Jul 2010.
- [22] N. M. Ferrers. *An Elementary Treatise on Spherical Harmonics and Subjects Connected with Them*. Macmillan and Co., London, 1877.
- [23] Kendall Atkinson and Weimin Han. *Spherical Harmonics and Approximations on the Unit Sphere: An Introduction*. Lecture Notes in Mathematics. Springer Berlin Heidelberg, Berlin, Heidelberg, 2012 edition, 2012.
- [24] Ram Dixit and Richard Cyr. Encounters between Dynamic Cortical Microtubules Promote Ordering of the Cortical Array through Angle-Dependent Modifications of Microtubule Behavior[W]. *The Plant Cell*, 16(12):3274–3284, 12 2004.
- [25] Xavier Lamy. Uniaxial symmetry in nematic liquid crystals. *Annales de l’Institut Henri Poincaré C, Analyse non linéaire*, 32(5):1125–1144, 2015.